Acta Crystallographica Section B
Structural Science
ISSN 0108-7681

Sodium carbonate revisited

Michal Dusek, Gervais Chapuis, Mathias Meyer and Vaclav Petricek

Acta Crystallographica Section B
Structural Science
ISSN 0108-7681

Sodium carbonate revisited

Michal Dusek,[a,b]* Gervais Chapuis,[b] Mathias Meyer[b] and Vaclav Petricek[a]

[a]Institute of Physics, Academy of Sciences of the Czech Republic, Na Slovance 2, 182 21 Praha, Czech Republic, and [b]Universite de Lausanne, Institut de Cristallographie, BSP Dorigny, CH-1015 Lausanne, Switzerland

Correspondence e-mail: dusek@fzu.cz

Received 7 January 2003
Accepted 22 April 2003

We present the structure of anhydrous sodium carbonate at room temperature (phase γ) and 110 K (phase δ) based on single-crystal X-ray diffraction data. The incommensurate phase γ was determined almost 30 years ago in the harmonic approximation using one modulation wave and first-order satellites. In our work we use satellites up to fifth order and additional harmonic waves to model the anharmonic features of the structure. The commensurate phase δ is presented for the first time. Using the superspace approach, both phases are compared in order to find common trends in the whole range of the sodium carbonate phases. We present arguments supporting the hypothesis that the driving force of the phase transitions may originate in the unsaturated bonding potential of one of the Na ions.

1. Introduction

Anhydrous Na_2CO_3 has been widely investigated over the past three decades from two basic points of view. First, its room-temperature phase is incommensurately modulated with very strong satellite reflections. Brouns *et al.* (1964) found that these spots could only be indexed if four indices were used. This discovery resulted in the foundation of the superspace approach by Janner, Janssen and de Wolff following the 9th International Crystallography Conference in Kyoto (Japan, 1973). Their approach recovers the periodic properties of modulated crystals by extending the basic crystallographic concepts to higher dimensional space. Na_2CO_3 was the first structure refined as a modulated structure in a harmonic approximation (de Wolff, 1974; van Aalst *et al.*, 1976).

The second point of view concerns the investigation of phase transitions. At high temperature (see Table 1), sodium carbonate undergoes a first phase transition from a hexagonal to a monoclinic structure. At room temperature an incommensurately modulated phase appears which transforms to a commensurate lock-in phase at low temperatures. In this article, the phases will be referred to as α, β, γ and δ starting from the hexagonal high-temperature phase. An overview is given in Table 1. The $\alpha \Rightarrow \beta$ hexagonal-to-monoclinic ferroelastic phase transition has been presented as an ideal system for lattice melting (Harris & Dove, 1995; Swainson *et al.*, 1995; Harris *et al.*, 1996).

In the present work we concentrate on the structure analysis of phases γ and δ. The structure of the incommensurate phase γ was previously solved in the harmonic

Table 1
Phases of Na_2CO_3.

Cell parameters given to two decimal places. T (K) are transition temperatures.

Phase	T (K)	Symmetry	Cell parameters (Å, °)	Reference
α	757	$P6_3/mmm$	9.02, 5.21, 6.50, 90, 90, 90†	Swainson *et al.* (1995)
β	628	$C2/m$	8.98, 5.25, 6.21, 90, 99.33, 90	Swainson *et al.* (1995)
γ	170	$C2/m(\alpha 0\gamma)$	8.92, 5.25, 6.05, 90, 101.35, 90	This article
δ		$P2_1/n$	8.90, 5.24, 6.00, 90, 101.87, 90	This article

† Transformed to the orthorhombic cell.

approximation using only first-order satellites. With the development of measurement techniques, higher-order satellites could be reliably measured up to order 4 using a laboratory X-ray diffractometer and even higher order using synchrotron radiation. Naturally the question arises what is the difference between the harmonic description using only one harmonic modulation wave and an anharmonic description combining more harmonic waves? Meyer *et al.* (1995) have already presented preliminary results at the Aperiodic'94 conference. Here we give the final structure model including the displacement modulation.

The existence of the $\gamma \Rightarrow \delta$ lock-in transition at low temperature was first reported by de Pater & Helmholdt (1979) and confirmed by Harris & Salje (1992). To our knowledge, the structure of phase δ has not yet been determined, probably owing to difficulties linked to the preparation of good single crystals of anhydrous sodium carbonate.

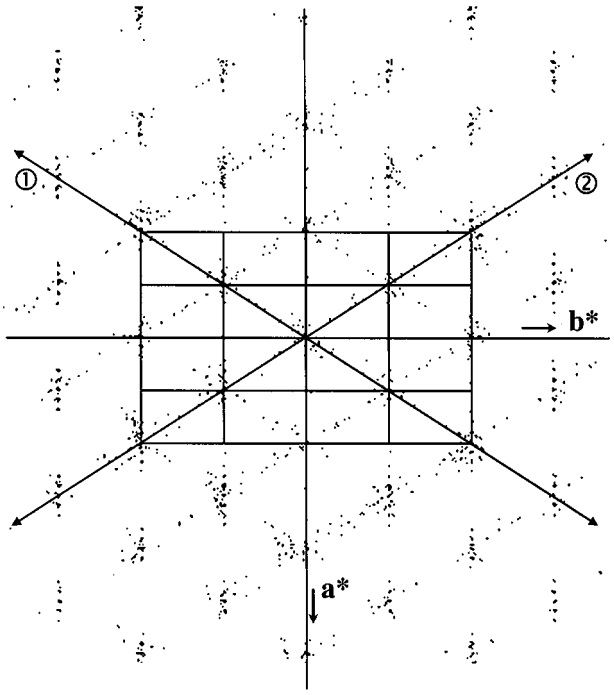

Figure 1
Projection of the reciprocal space of phase γ along **c***. Strong peaks are represented by dots; the satellite reflections are projected in the **a***, **b*** plane. The peaks that can neither be indexed as a main reflection nor as satellites are mostly located along the dotted lines labelled '1' and '2' (in rings). This indicates the presence of two other domains of Na_2CO_3.

2. Experimental

2.1. Preparation

Reagent-grade anhydrous sodium carbonate was placed in the tube of a Bridgeman apparatus. At a temperature of 723 K the heater system was raised at a speed of 1 mm per day. The single crystal grown was kept in an open phial under dry nitrogen over a molecular sieve. This phial was subsequently transferred into a glovebox with less than 10 p.p.m. of water vapour. In this box the crystal was shattered into smaller chips, which were then placed into the Enraf sample grinder. While constantly monitoring the development of the grinding process by means of a binocular built into the wall of the glovebox, some suitable, but somewhat egg-shaped, samples could be obtained for diffraction. These were then gently jostled into borosilicate capillaries and made to stick on their walls by a small film of degassed silicon grease. Finally, these capillaries were sealed inside the glovebox by means of a CO_2 laser.

2.2. Data collection

Details of the measurements are summarized in Table 2.[1] All measurements were carried out using a Kuma four-circle diffractometer equipped with a CCD detector and a cryostream cooling device. Measurement was carried out with a detector distance of 71 mm and with 0.5° ω and φ oscillation steps to a 2θ angle up to 70°. Many of the reflections were multiply measured. The exposure time was from 25 to 60 s depending on the detector angle. In the reciprocal space viewer, the peak positions revealed that the crystal contained an admixture of other domains (see Fig. 1) with weaker intensities. Fortunately, they did not overlap with the main domain which could be integrated independently.

The absorption was neglected because the egg-shaped crystal within the capillary did not allow any reliable indexing. Later, a comparison of the results for data without absorption correction and data corrected for an approximate shape described with many faces gave the same results. For the data processing and reciprocal space reconstructions, the *RED* software (Kuma Diffraction, 2000; Oxford Diffraction, 2001) was used. The modulation wavevector was refined with the program *NADA* (Schönleber *et al.*, 2001). The diffraction pattern of phase γ is shown in Fig. 2. In accordance with unpublished synchrotron measurement (Lam, 1998), which revealed satellites up to sixth order, the data integration was performed up to $m = 6$. However, only 49 sixth-order satellites above the limit of 3σ were detected. Thus, the sixth-order satellites were neglected in the refinement. The fifth-order satellites were used to check their fit with the tested structure

[1] Supplementary data for this paper are available from the IUCr electronic archives (Reference: SN0033). Services for accessing these data are described at the back of the journal.

Table 2
Experimental data.

δ-Na_2CO_3: (1) superspace description; (2) sixfold supercell description.

	γ -Na_2CO_3	δ-Na_2CO_3 (1)	δ-Na_2CO_3 (2)
Crystal data			
Chemical formula	Na_2CO_3	Na_2CO_3	Na_2CO_3
Temperature (K)	295	110	110
Cell setting	Monoclinic	Monoclinic	Monoclinic
(Super)space group	$C2/m(\alpha 0\gamma)0s$	$C2/m(\alpha 0\gamma)0s$	$P2_1/n$
a (Å)	8.920 (7)	8.898 (7)	19.91 (2)
b (Å)	5.245 (5)	5.237 (5)	5.237 (6)
c (Å)	6.050 (5)	5.996 (5)	17.99 (2)
γ (°)	101.35 (8)	101.87 (8)	119.01 (5)
V (Å^3)	277.5 (8)	273.4 (8)	1641 (6)
Formula units	4	4	24
(Mg m^{-3})	2.536	2.574	2.574
Modulation wavevector	[0.182 (1), 0, 0.322 (1)]	(1/6,0,1/3)	–
Crystal form	Irregular, without natural planes	Irregular, without natural planes	Irregular, without natural planes
Crystal size (mm^3)	0.4	0.4	0.4
Crystal colour	White	White	White
Data collection			
Diffractometer	KUMA CCD	KUMA CCD	KUMA CCD
Radiation type	Mo $K\alpha$	Mo $K\alpha$	Mo $K\alpha$
Wavelength	0.71073	0.71073	0.71073
Absorption correction type	None	None	None
μ (mm^{-1})	0.491	0.499	0.499
Range of h, k, l, m, n	$-18 \Rightarrow h \Rightarrow 18$	$-18 \Rightarrow h \Rightarrow 18$	$-40 \Rightarrow h \Rightarrow 40$
	$-10 \Rightarrow k \Rightarrow 10$	$-10 \Rightarrow k \Rightarrow 10$	$-10 \Rightarrow k \Rightarrow 10$
	$-12 \Rightarrow l \Rightarrow 12$	$-12 \Rightarrow l \Rightarrow 11$	$-36 \Rightarrow l \Rightarrow 33$
	$-6 \Rightarrow m \Rightarrow 6$	$-3 \Rightarrow m \Rightarrow 3$	–
No. of measured reflections	77 868	61 103	61 101
No. of unique reflections	14 118	12 347	12 347
No. of observed reflections	4178	5695	5695
No. of main reflections	1155	2163	12 347
No. of observed first-order satellites	1244	1901	–
No. of observed second-order satellites	1033	1869	–
No. of observed third-order satellites	595	837	–
No. of observed fourth-order satellites	330	–	–
No. of observed fifth-order satellites	113	–	–
No. of observed sixth-order satellites	49	–	–
Criterion for observed reflections	$I > 3\sigma(I)$	$I > 3\sigma(I)$	$I > 3\sigma(I)$
R_{int} (all reflections)	0.0641	0.0672	0.0672
R_{int} (main reflections)	0.046	0.056	–
$R_{int,all}$, $R_{int,obs}$ (first-order satellites)	0.055, 0.050	0.066, 0.057	–
$R_{int,all}$, $R_{int,obs}$ (second-order satellites)	0.106, 0.075	0.116, 0.078	–
$R_{int,all}$, $R_{int,obs}$ (third-order satellites)	0.274, 0.137	0.156, 0.103	–
$R_{int,all}$, $R_{int,obs}$ (fourth-order satellites)	0.727, 0.234	–	–
$R_{int,all}$, $R_{int,obs}$ (fifth-order satellites)	1.211, 0.375	–	–
$R_{int,all}$, $R_{int,obs}$ (sixth-order satellites)	1.396, 0.562	–	–
Refinement			
Refinement on	F	F	F
R_{all}, wR_{all}	0.181, 0.069	0.117, 0.075	0.115, 0.071
R_{obs}, wR_{obs}	0.045, 0.060	0.045, 0.066	0.043, 0.062
R_{obs}, R_{all}, wR_{all} (main reflections)	0.035, 0.050, 0.062	0.040, 0.079, 0.076	–
R_{obs}, R_{all}, wR_{all} (first-order satellites)	0.034, 0.071, 0.042	0.040, 0.102, 0.064	–
R_{obs}, R_{all}, wR_{all} (second-order satellites)	0.053, 0.153, 0.059	0.055, 0.162, 0.080	–
R_{obs}, R_{all}, wR_{all} (third-order satellites)	0.080, 0.294, 0.105	0.067, 0.179, 0.088	–
R_{obs}, R_{all}, wR_{all} (fourth-order satellites)	0.111, 0.490, 0.159	–	–
R_{obs}, R_{all}, wR_{all} (fifth-order satellites)	0.222, 0.664, 0.407	–	–
R_{obs}, R_{all}, wR_{all} (sixth-order satellites)	0.786, 0.831, 0.821	–	–
S_{obs}, S_{all}	2.42, 1.50	1.71, 1.31	1.64, 1.26
No. of parameters	180	205	325
Weighting scheme	$w = [\sigma^2(F) + (0.01F)^2]^{-1}$	$w = [\sigma^2(F) + (0.01F)^2]^{-1}$	$w = [\sigma^2(F) + (0.01F)^2]^{-1}$
$(\Delta/\sigma)_{max}$	0.0002	0.0029	0.0015
$\Delta\rho_{max}$ (e Å^{-3})	0.54	0.69	0.67
$\Delta\rho_{min}$ (e Å^{-3})	-0.60	−0.64	−0.59
Extinction correction	None	$\Delta\rho_{max}$	$\Delta\rho_{max}$

Computer programs used: *JANA*2000 (Petricek & Dusek, 2000), *NADA* (Schönleber *et al.*, 2001), *RED* (Kuma Diffraction, 2000; Oxford Diffraction, 2001).

models despite their poor reliability (see values of $R_{\rm int}$ in Table 2).

3. Superspace description of commensurate structures

The superspace approach to describe commensurate structures has been used for a long time and the underlying theory is given in Dam & Janner (1986). Its growing use (see, for instance, Evain *et al.*, 1998; Bagautdinov *et al.*, 1999; Lambert *et al.*, 2002) is related to the implementation of the method and its automation in the software program *JANA*2000 (Petricek & Dusek, 2000). It is now used by scientists who are not specialists in aperiodic crystallography. The relatively straightforward case of the δ phase of Na_2CO_3 is an excellent opportunity to explain the method, especially from the practical point of view.

Satellite reflections of commensurate structures can be indexed using a $\mathbf{q}$ vector with rational components, $\mathbf{q} = \left(\frac{1}{n_1}, \frac{1}{n_2}, \frac{1}{n_3}\right)$. Assuming that the integers n_1, n_2 and n_3 are small, the structure can be equally well solved and described with an N-fold supercell, $N \leq n_1 \times n_2 \times n_3$. Later in this section we shall see that the superspace description has some advantages.

The atomic positions in a one-dimensionally modulated structure are given as the sum of an average position and a shift

$$x_i^\mu = \overline{x}_i^\mu + u_i^\mu(\overline{x}_4),$$
$$\overline{x}_i^\mu = L_i + \overline{x}_i^{0\mu},$$
$$\overline{x}_4 = t + \mathbf{q}\cdot\mathbf{x},$$

where $(\overline{x}_i^\mu,\ i = x, y, z)$ are the coordinates of atom μ in the average structure, L_i are integers and $\overline{x}_i^{0\mu}$ the average position within the unit cell. The components of the modulation function of atom μ are $u_i^\mu(\overline{x}_4)$ with $u_i(\overline{x}_4 + 1) = u_i(\overline{x}_4)$. $\overline{x}_4 = t_0 + \mathbf{q}\cdot\mathbf{x}$ is the fourth (superspace) coordinate with starting phase t_0.

For incommensurately modulated structures $\overline{x}_4$ can take all possible values between 0 and 1. In a commensurate structure, however, the modulation function is defined only at points corresponding to the N positions of the relevant atom in an N-fold superstructure. Fig. 3 illustrates an example of a sixfold superstructure which is found in phase δ of sodium carbonate. The shaded area is the four-dimensional supercell $\mathbf{A}_3$, which represents the first three coordinates of the superspace, and $\mathbf{A}_4$ is the fourth coordinate. The horizontal dotted lines denote the real space section t_0 through the superspace, which is used for the description of our superstructure, and all its equivalents following from the translation periodicity. The wavy line in the figure denotes the modulation function; its definition points correspond to the intersections with the lines t_0. Owing to the sixfold nature we can find six non-equivalent intersections. Assuming that the modulation function describes atomic positions, the intersections define six different positions, C_1,C_2, .., C_6, of the atom in the supercell.

The section t_0 can be arbitrarily shifted along $\mathbf{A}_4$. The shift changes the positions C_i, *i.e.* it changes the resulting superstructure. The symmetry of the superstructures generated for various values of t_0 can be derived from the superspace group of the commensurate structure. The selection of the best t_0 yielding the best fit between the observed and calculated

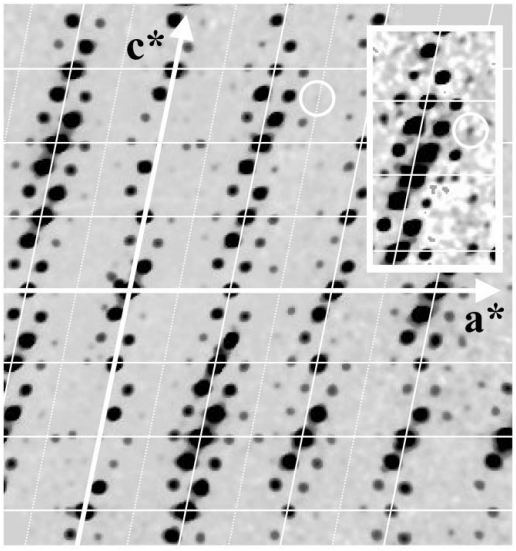

Figure 2
Reconstruction of the reciprocal plane *h*2*l* in γ -sodium carbonate. The intersections of dotted and solid white lines correspond to main reflections systematically absent as a result of the C centering. The white circle shows the position of the fifth-order satellite 2215. This reflection is visible in the insert showing the corresponding area on a different scale.

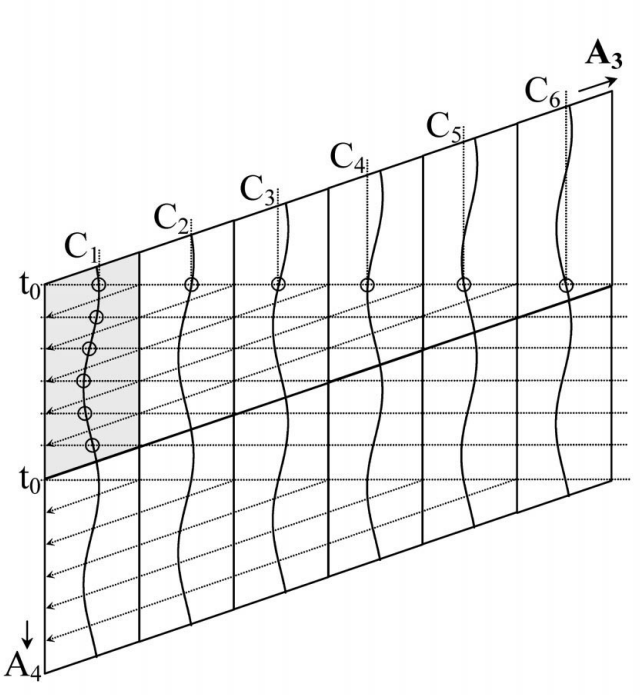

Figure 3
Schematic representation of a sixfold commensurate structure showing the influence of the choice of t_0 on the resulting superstructure. The open circles represent points where the modulation function is defined.

Table 3
Displacement parameters in the average structure of γ-Na_2CO_3.

	U^{11}	U^{22}	U^{33}	U^{12}	U^{13}	U^{23}
Na1	0.0155 (11)	0.071 (2)	0.0162 (12)	0	0.0054 (10)	0
Na2	0.0179 (12)	0.095 (3)	0.0162 (12)	0	0.0077 (11)	0
Na3	0.0213 (11)	0.116 (3)	0.0306 (14)	0	0.0100 (11)	0
C	0.0088 (13)	0.073 (3)	0.0107 (15)	0	0.0021 (12)	0
O1	0.083 (3)	0.137 (4)	0.066 (2)	−0.081 (3)	0.053 (3)	−0.045 (3)
O2	0.0159 (11)	0.0352 (14)	0.0247 (14)	0	0.0115 (11)	0

Table 4
Final coordinates, equivalent isotropic displacement parameters and Fourier amplitudes of the displacive modulation functions for γ-Na_2CO_3.

The waves are sorted by the term (s for sinus, c for cosinus) and n.

	Wave	x	y	z	U_{eq} (Å^2)
Na1		0	0	0	0.01731 (11)
	s,1	0	0.05527 (10)	0	
	c,1	0	0	0	
	s,2	0.00178 (6)	0	0.00108 (8)	
	c,2	0	0	0	
	s,3	0	−0.00490 (9)	0	
	c,3	0	0	0	
	s,4	−0.00135 (7)	0	−0.00101 (13)	
	c,4	0	0	0	
Na2		0	0	0.5	0.01673 (11)
	s,1	0	0.06238 (9)	0	
	c,1	0	0	0	
	s,2	0.00057 (6)	0	−0.00187 (8)	
	c,2	0	0	0	
	s,3	0	0.00452 (9)	0	
	c,3	0	0	0	
	s,4	0.00071 (8)	0	−0.00017 (13)	
	c,4	0	0	0	
Na3		0.17055 (4)	0.5	0.74801 (6)	0.02554 (10)
	s,1	0	0.06581 (8)	0	
	c,1	0	−0.00518 (8)	0	
	s,2	−0.00103 (4)	0	−0.00114 (7)	
	c,2	0.00151 (5)	0	0.00464 (7)	
	s,3	0	0.00131 (7)	0	
	c,3	0	−0.00388 (7)	0	
	s,4	0.00192 (6)	0	0.00129 (11)	
	c,4	0.00111 (6)	0	0.00028 (11)	
C		0.16446 (7)	0.5	0.24914 (10)	0.01155 (13)
	s,1	0	0.05693 (13)	0	
	c,1	0	−0.00087 (13)	0	
	s,2	0.00073 (9)	0	−0.00192 (14)	
	c,2	0.00079 (9)	0	−0.00093 (13)	
	s,3	0	0.00103 (14)	0	
	c,3	0	0.00540 (14)	0	
O1		0.10159 (5)	0.29384 (7)	0.28535 (7)	0.02607 (12)
	s,1	−0.02589 (7)	0.07376 (9)	−0.02096 (10)	
	c,1	−0.01640 (6)	0.00289 (9)	−0.03486 (9)	
	s,2	0.00113 (6)	0.00191 (9)	−0.00124 (9)	
	c,2	0.00018 (6)	0.00006 (9)	−0.00207 (9)	
	s,3	0.00169 (7)	0.00030 (8)	0.00249 (10)	
	c,3	−0.00542 (6)	0.00941 (8)	−0.00255 (9)	
	s,4	0.00025 (8)	0.00058 (11)	0.00023 (14)	
	c,4	0.00045 (8)	0.00063 (11)	−0.00005 (13)	
O2		0.28987 (6)	0.5	0.17757 (11)	0.02274 (14)
	s,1	0	0.02301 (14)	0	
	c,1	0	−0.00790 (14)	0	
	s,2	0.00060 (7)	0	−0.00273 (11)	
	c,2	0.00177 (7)	0	0.00004 (11)	
	s,3	0	0.00204 (12)	0	
	c,3	0	−0.00271 (12)	0	
	s,4	−0.00077 (9)	0	−0.00039 (17)	
	c,4	−0.00012 (10)	0	−0.00123 (18)	

structure factors is the basic task of the structure analysis of commensurate crystals.

The advantage of this approach over the classical three-dimensional refinement relates to the ease of testing various superstructures with different symmetry using the same cell parameters, data set and superspace symmetry, by merely redefining t_0. In the commensurate refinement, the number of refined parameters can also be more conveniently controlled in terms of the number of modulation waves. For instance, we can add ADP modulation waves (ADP = atomic displacement parameters) for some atoms as long as they significantly improve the fit. If at this stage the maximum number of displacement parameters is not reached this means they are similar or dependent in the superstructure. This fact cannot be described with temperature ellipsoids in a three-dimensional refinement. The superspace refinement is also very useful for the systematic description of crystal structures, using a unified approach for commensurate and incommensurate phases.

4. Structure analysis

4.1. Refinement of incommensurate γ-Na_2CO_3

The reflections of γ-Na_2CO_3 were indexed using four indices and the vector **q** given in Table 2. As *JANA*2000 (Petricek & Dusek, 2000) enables switching between 3*d* and 4*d* structures, the same data set was used for the refinement of both the average and the modulated structure. Only observed reflections up to fifth-order satellites were used. The sixth-order satellites were excluded from the refinement because of their weakness.

4.1.1. Average structure. The refined parameters of the average structure are close to the previously published values (van Aalst *et al.*, 1976). With anisotropic displacement factors for all atoms, the refinement converged to R = 0.12 for 814 observed main reflections. This refinement provided a good starting model for the modulated structure refinement. Large values of some displacement parameters, especially U^{22} (see Table 3), indicated which atoms were most affected by the modulation, in excellent agreement with the refinement of the modulated structure presented below.

4.1.2. Modulated structure. The results of the modulated structure refinement are given in Tables 4 and 5. Small arbitrary starting values of the first position modulation wave were assigned to the starting model. The refinement converged smoothly with the fit given in Table 6. The first wave suitably reproduces only the first-order satellites. With four position modulation waves for all atoms except carbon, where three waves sufficiently describe its displacement, the fit of the first- and second-order satellites was already quite satisfactory, while the higher-order satellites were at odds with our structure model. The Fourier maps (Fig. 4) clearly indicated that

the refinement of ADP modulation could improve the fit. Additional ADP modulation waves were introduced one by one for each atom until they improved significantly both the R values and the relevant difference Fourier sections. Large differences between atoms were found, from C atoms without ADP modulation to O atoms where three ADP modulation waves were necessary. In the final model the modulation functions fitted very well with the Fourier maxima. The corresponding difference Fourier section (Fig. 4), plotted with steps of 0.1 e Å^{-3}, was virtually flat despite the fact that this illustration concerns the O1 atom with the most complex modulation behaviour.

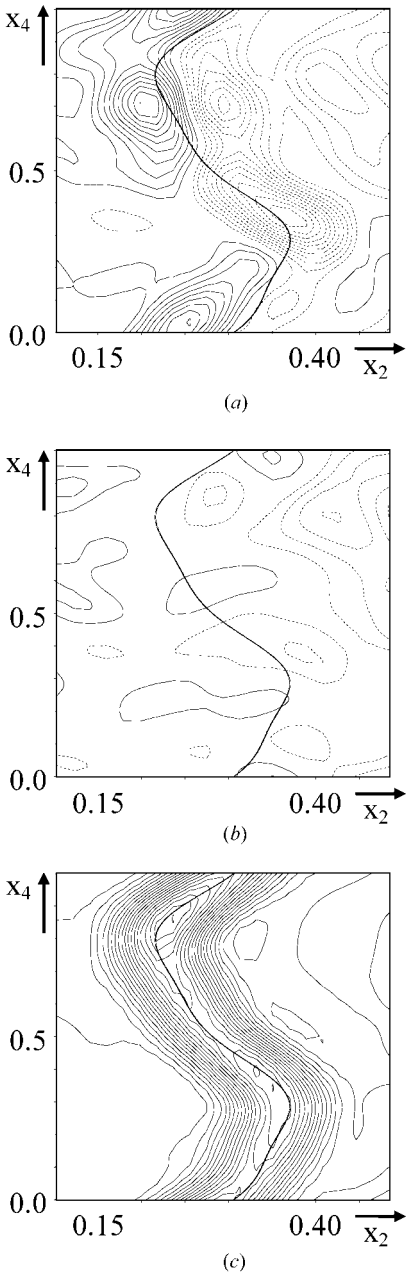

Figure 4
Fourier section x_4–x_2 through the O1 atom of γ-Na_2CO_3. (*a*) $F_o - F_c$ map without ADPmodulation; (*b*) $F_o - F_c$ map of the final structure model; (*c*) F_o map of the final structure model. The contour step is 0.1 e Å^{-3} for (*a*) and (*b*), and 1.0 e Å^{-3} for (*c*). The dashed lines indicate negative densities.

4.2. Commensurate δ-Na_2CO_3

The δ phase was indexed with four indices using the vector **q** = (1/6,0,1/3) with an elementary cell very close to phase γ. The average structure of phase γ was taken as a starting point for the commensurate refinement. By adding and refining the modulation waves for a given t_0 and superspace symmetry we could create structure models of the possible commensurate structures.

4.2.1. Transformation relating the supercell and superstructure description. The straightforward transformation from the superspace description to the supercell yields the 18-fold 6 × 1 × 3 superstructure using the transformation (applicable to reciprocal cell parameters as column vectors)

$$\mathbf{T}_1 = \begin{pmatrix} \frac{1}{6} & 0 & 0 \\ 0 & 1 & 0 \\ 0 & 0 & \frac{1}{3} \end{pmatrix}.$$

The **q** × **l** products, where **l** is an integer translation, in Fig. 5 indicate that the 18-fold superstructure consists of three identical sixfold parts and that it can be fully described either by a 6 × 1 × 1 or 2 × 1 × 3 supercell. In this refinement we used the 6 × 1 × 1 supercell for the commensurate structure. However, the following transformation was selected to convert the refinement results into the supercell

$$\mathbf{T}_3 = \begin{pmatrix} \frac{1}{2} & 0 & 0 \\ 0 & 1 & 0 \\ \frac{1}{6} & 0 & \frac{1}{3} \end{pmatrix}.$$

This yields an equivalent sixfold supercell with improved indexing with $\mathbf{c}^*$ parallel to the **q** vector (see Fig. 6). The direct space transformation from the 6 × 1 × 3 supercell to the actual supercell is

$$\mathbf{T}_3 = \begin{pmatrix} \frac{1}{3} & 0 & 0 \\ 0 & 1 & 0 \\ -\frac{1}{3} & 0 & 1 \end{pmatrix}.$$

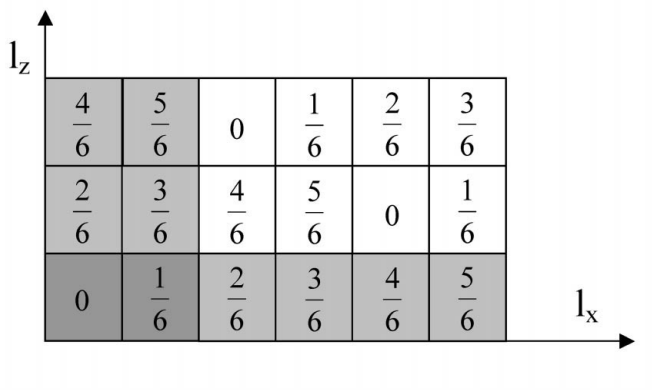

Figure 5
The products, where **l** is an integer translation (l_x,0,l_z) and **q** is the incommensurate vector of γ-Na_2CO_3.

Table 5
Final displacement parameters and ADP modulation functions for γ-Na_2CO_3.

The waves are sorted by the term (s for sinus, c for cosinus) and *n*.

	Wave	U^{11}	U^{22}	U^{33}	U^{12}	U^{13}	U^{23}
Na1		0.01757 (18)	0.01860 (15)	0.01713 (19)	0	0.00672 (16)	0
	s,1	0	0	0	0	0	0
	c,1	0	0	0	−0.00082 (16)	0	−0.00157 (17)
	s,2	0	0	0	0	0	0
	c,2	−0.0022 (3)	0.0007 (2)	−0.0009 (3)	0	−0.0007 (2)	0
Na2		0.01919 (19)	0.01561 (15)	0.01686 (19)	0	0.00714 (17)	0
	s,1	0	0	0	0	0	0
	c,1	0	0	0	0.00040 (17)	0	−0.00027 (17)
	s,2	0	0	0	0	0	0
	c,2	0.0000 (3)	0.0015 (2)	0.0007 (3)	0	0.0006 (2)	0
Na3		0.02174 (16)	0.02568 (14)	0.0307 (2)	0	0.00888 (16)	0
	s,1	0	0	0	0.00035 (14)	0	−0.00157 (15)
	c,1	0	0	0	0.00441 (15)	0	0.00155 (16)
	s,2	0.0005 (2)	0.00111 (18)	−0.0005 (2)	0	−0.00017 (19)	0
	c,2	0.0005 (2)	0.00302 (18)	0.0004 (2)	0	0.00053 (19)	0
C		0.0111 (2)	0.01219 (17)	0.0119 (2)	0	0.0037 (2)	0
O1		0.0318 (2)	0.01881 (14)	0.0299 (2)	−0.00956 (13)	0.01172 (18)	0.00055 (13)
	s,1	−0.0036 (3)	0.0027 (2)	0.0019 (3)	−0.00305 (18)	−0.0014 (3)	−0.00124 (19)
	c,1	−0.0072 (3)	0.0017 (2)	0.0013 (3)	−0.00030 (18)	−0.0010 (3)	−0.00233 (18)
	s,2	−0.0043 (3)	−0.00197 (19)	−0.0049 (3)	0.00282 (18)	−0.0039 (2)	0.00191 (19)
	c,2	0.0020 (3)	0.00276 (19)	−0.0026 (3)	−0.00256 (19)	−0.0001 (2)	−0.00166 (19)
	s,3	0.0016 (3)	−0.0002 (2)	−0.0004 (4)	0.0000 (2)	−0.0003 (3)	0.0012 (2)
	c,3	−0.0017 (3)	0.0015 (2)	0.0005 (4)	−0.0007 (2)	−0.0003 (3)	−0.0002 (2)
O2		0.0148 (2)	0.0324 (3)	0.0237 (3)	0	0.0104 (2)	0
	s,1	0	0	0	0.0057 (2)	0	0.0035 (3)
	c,1	0	0	0	−0.0018 (2)	0	0.0000 (3)
	s,2	−0.0011 (3)	−0.0034 (3)	−0.0016 (4)	0	−0.0009 (3)	0
	c,2	−0.0016 (3)	0.0007 (3)	−0.0007 (4)	0	−0.0012 (3)	0
	s,3	0	0	0	0.0006 (3)	0	0.0002 (3)
	c,3	0	0	0	0.0021 (3)	0	0.0013 (3)

Table 6
The fit between observed and calculated data of γ-Na_2CO_3 for 4129 reflections exceeding $3\sigma(I)$ using different structure models.

In Model 1 only one position modulation wave was refined. Model 2 uses the final set of position modulation parameters. Model 3 is identical to our final results. *N* represents the number of parameters.

Model	*S*	R_{all}	R_{main}	R_1	R_2	R_3	R_4	*N*
1	8.92	0.1321	0.0670	0.1017	0.2059	0.2995	0.6113	50
2	3.65	0.0693	0.0504	0.0649	0.0847	0.1185	0.1882	104
3	2.32	0.0433	0.0354	0.0340	0.0527	0.0795	0.1335	180

4.2.2. Number of parameters. In the commensurate structure the modulation functions are completely described by a finite Fourier expansion. In the superspace refinement, the same maximal number of parameters can be used as in a conventional refinement in the supercell. With the same number of parameters both descriptions are equivalent.

The number of parameters for the superspace refinement can be derived from simple considerations. On a general position of the basic structure an atom generates *N* atoms in the superstructure. *N* is minimally equal to the order of the superstructure (6 in our case). This number increases further by lowering the superstructure symmetry. For instance, in the superspace group $C2/m(\alpha 0\gamma)0s$, with $t_0 = 1/5$, the space-group symmetry of the sixfold superstructure is *Pn*, giving rise to 12 positions from each general position in the basic structure. The maximal number of position parameters refined for the atom in the supercell is $3N$. In the superspace description we can therefore refine the basic position (three parameters) plus $3N - 3$ for position modulation parameters. Using the same arguments, we can refine $6N$ displacement parameters in the supercell, which is equivalent to six displacement parameters of the corresponding basic position plus $6N - 6$ of the ADP modulation parameters. From the last wave we can use either cos or sin terms. Atoms in special positions must be treated individually.

4.2.3. Refinement. Table 7 lists the space groups in the 18-fold superstructure compatible with the possible superspace groups using various values of t_0. Here it should be noted that following the transformation to the sixfold superstructure, the space-group symbols change owing to the choice of unit cell. For instance, $P2_1/a$ becomes $P2_1/n$ *etc*. According to our expectations, the refinement confirmed that a reasonable fit between observed and calculated data could only be obtained in the superspace group $C2/m(\alpha 0\gamma)0s$, as in phase γ, using t_0 values of 0, 1/8 and 1/5 corresponding to space groups $P2/n$, $P2_1/n$ and *Pn* in the sixfold supercell. The refinement results for the three cases are summarized in Table 8. From this table it is clear that the correct model is that for $t_0 = 1/8$. With $t_0 = 0$ the results were significantly worse, whereas the lower

Table 7
Space groups of the 18-fold superstructure derived from the possible superspace groups of δ-Na_2CO_3.

	$t = n(\frac{1}{12})$	$t = (2n+1)(\frac{1}{24})$	Other values of t
$C2/m(\alpha 0\gamma)0s$	$P2/a$	$P2_1/a$	Pa
$C2/m(\alpha 0\gamma)$	$P2/m$	$P2_1/m$	Pm
$Cm(\alpha 0\gamma)s$	Pa	Pa	Pa
$Cm(\alpha 0\gamma)$	Pm	Pm	Pm
$C2(\alpha 0\gamma)$	$P2$	$P2_1$	$P1$

symmetry group associated with $t_0 = 1/5$ did not improve the results.

In the next step we tested for the minimal set of parameters necessary to describe the structure. We used the maximum number of position waves for all atoms except carbon, where the sixth position wave did not improve the R factor. The final position parameters are listed in Table 9. With the ADP modulation parameters (Table 10) the conditions were different, as only O1 required more than two waves to describe the ADP modulation. For Na1, Na2 and C the ADP modulation was not required. This indicates that their displacement parameters for particular positions in the superstructure should be very similar. In Table 11 the fit between observed and calculated data for the full and the reduced set of ADP modulation parameters is compared with a structure model without ADP modulation. A reduction of 126 parameters, corresponding to the change from the full set to the reduced one, increased the R value by 0.23%, whereas removing the remaining 72 ADP modulation parameters caused an additional rise of 1.35%. The model with the reduced set of displacement parameters was therefore used as the final commensurate structure. The sixfold superstructure given in Table 12 was refined with a full set of displacement parameters, as is usual in the standard refinement.

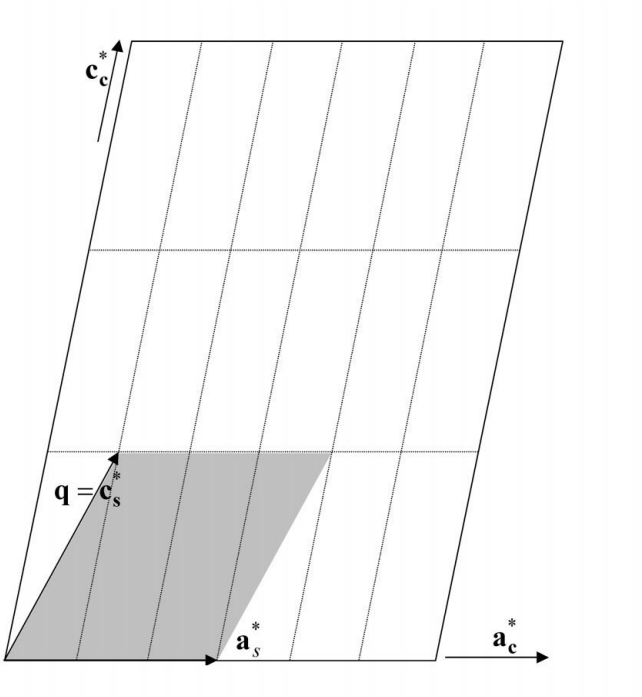

Figure 6
Relation between the commensurate cell and the sixfold supercell (shaded) used in this article. The subscripts 'c' and 's' indicate the commensurate and the supercell description.

5. Discussion

The modulation of phase γ has been described by van Aalst *et al.* (1976) in the harmonic approximation. de Wolff & Tuinstra (1986) thoroughly discussed the crystal geometry of the α, β

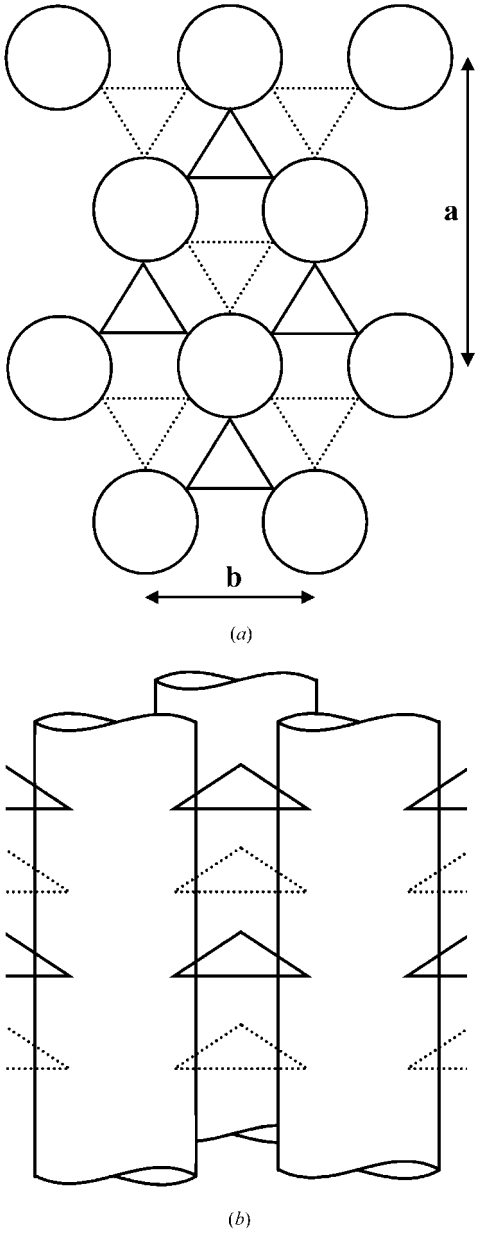

Figure 7
Schematic description according to Harris & Dove (1995) of α- and β-sodium carbonate. The columns approximate the shape of NaO_6 octahedra. The CO_3 groups are represented by triangles; the solid and dashed lines denote the different height of the CO_3 groups. (*a*) Projection of the hexagonal phase α along **c** with cross sections (rings) through the NaO_6 columns. (*b*) Projection of phase β along **a**. The rear NaO_6 column is shifted up because of the shear strain.

and γ phases. We shall focus on the comparison between the harmonic and anharmonic description of phase γ. From a geometrical point of view, the newly determined phase δ, although very similar to phase γ, will help us to understand the role of the sodium ion $Na3^+$ (see later) in the sequence of phase transitions.

5.1. Phase transitions in sodium carbonate in terms of shear strain

In this paragraph we shall briefly repeat the main points from de Wolff & Tuinstra (1986) as they are necessary to understand the structure of sodium carbonate. The high-temperature α phase is hexagonal (Table 1) with symmetrically independent atoms C, O, Na1 and Na2. Na1 forms a rather rigid face-sharing $Na1O_6$ octahedron giving rise to columns along the hexagonal axis. The columns are bound together with rigid CO_3 groups. Another sodium atom, Na2, lies between two adjacent CO_3 groups occupying a site that is considerably larger than Na1. A schematic view of phase α is given in Fig. 7a.

At the α to β phase transition, a shear strain occurs which shifts adjacent NaO_6 columns along the former hexagonal **c** axis (see Fig. 7*b*). The symmetry of the structure changes to monoclinic with symmetrically independent atoms C, O1, O2, Na1, Na2 and Na3. In the two independent $Na1O_6$ and $Na2O_6$ octahedra, the bond distances are almost the same as in phase α.

Phases γ and δ preserve the overall features of phase β. Both exhibit the same symmetrically independent atoms and the superspace group is derived from the space group of phase β. The most characteristic feature is the flexing of the NaO_6 columns (see Fig. 8). The rigidity of the main building units is, however, retained.

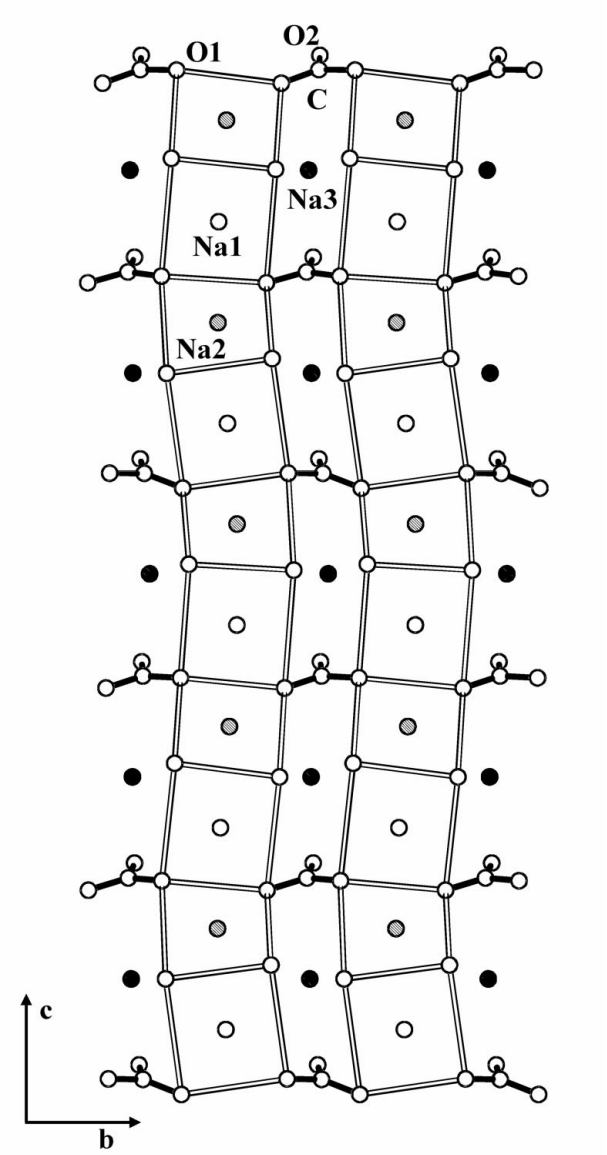

Figure 8
Projection of phase γ along **a**. The double lines reflect the shape of the NaO_6 columns shown in Fig. 7. The black thick lines denote the chemical bonds in the CO_3^{2-} ions. Ions $Na1^+$ (white circles) and $Na2^+$ (hatched circles) are at the center of the octahedra; their bonds are not plotted. In addition to the four neighbouring O1 atoms, they are bonded to two other O2 atoms (not shown here) that connect the columns through other CO_3^{2-} groups with columns above and below the plane of the plot. The $Na3^+$ ions (black circles) lie outside of the NaO_6 octahedra between adjacent CO_3^{2-} groups.

5.2. Single-atom modulations

The position modulations of phases γ and δ are given in Tables 4 and 9, respectively. The O1 atom exhibits the largest displacements with amplitudes of 0.2, 0.4 and 0.2 Å along the **a**, **b** and **c** axes. The modulation of the other atoms occurs mainly in the **b** direction, with modulation functions often deviating far from the harmonic description (Fig. 9). The modulation amplitudes of the least modulated atom O2 are approximately 0.1 Å. In phase δ the definition points of the modulation functions are in good agreement with the functions of phase γ, indicating that both phases are very similar. The largest modulation of the displacement parameters (see Tables 5 and 10 for phases γ and δ, respectively) was found for

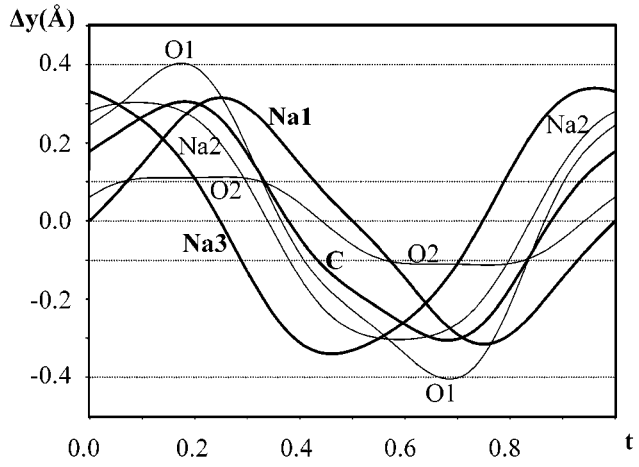

Figure 9
Modulation amplitudes along **b** in γ-sodium carbonate. The curves plotted with thick lines are labelled with bold letters.

atoms O1, O2 and Na3. In O1 the amplitudes are 0.011, 0.006 and 0.007 Å^2 for U^{11}, U^{22} and U^{33}, respectively, while for O2 and Na3 the most significant parameter is U^{22} with an amplitude of $\sim$ 0.004 Å^2. Both modulation amplitudes and the absolute values of the displacement parameters are significantly lower in phase δ, especially for O1, with a modulation amplitude U^{11} reduced to 0.006 Å^2. The equivalent isotropic displacement parameters are compared in Fig. 10 for phases γ and δ.

5.3. Rigidity of CO_3 and NaO_6 building units in phases γ and δ

Table 13 lists the bond lengths and angles of the CO_3^{2-} ions. In both phases, the CO_3^{2-} ions are rigid with less than 0.01 Å variation for bond lengths and 1° for angles. It should be noted here that all refinements have been carried out without restricting the bond lengths and angles.

In CO_3^{2-} ions the C—O distances should be in the range 1.29 $\pm$ 0.01 Å. Based on many observations, any significant deviation from this value indicates a failure of the model rather than reality. However, the distances of phase α based on coordinates from Swainson *et al.* (1995) are significantly shorter, $\sim$ 1.19 Å, with a corresponding unreasonably high bond-valence sum of $\sim$ 5.2 (Table 14). In phase β the bond-valence sum decreases to 4.43, which is still far from the expected value of 4.00. Moreover, the bond lengths differ for C—O1 and C—O2. de Wolff & Tuinstra (1986) have attributed these discrepancies to the strong anharmonic displacement which inhibits the precise calculation of distances. Indeed, in phase γ where the displacement parameters are reasonable, the C—O distance exhibits the standard value of 1.28 Å. In phase δ another decrease in the displacement parameter occurs (Fig. 10) and the C—O distance reaches its ideal value of 1.29 Å.

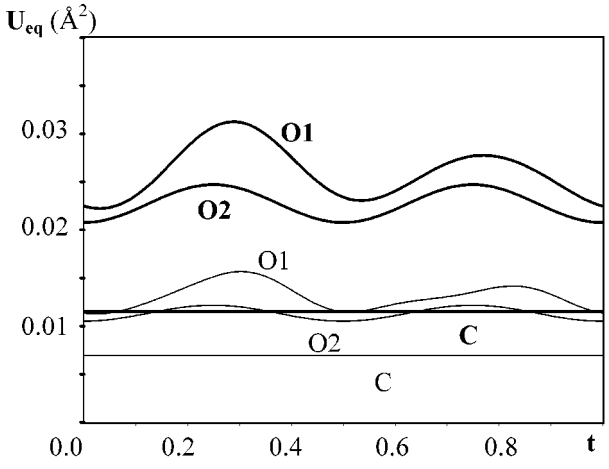

Figure 10
Equivalent isotropic displacement factors of atoms in the CO_3 group as a function of the internal coordinate *t*. The thick lines belong to phase γ, the others represent U_{eq} of phase δ.

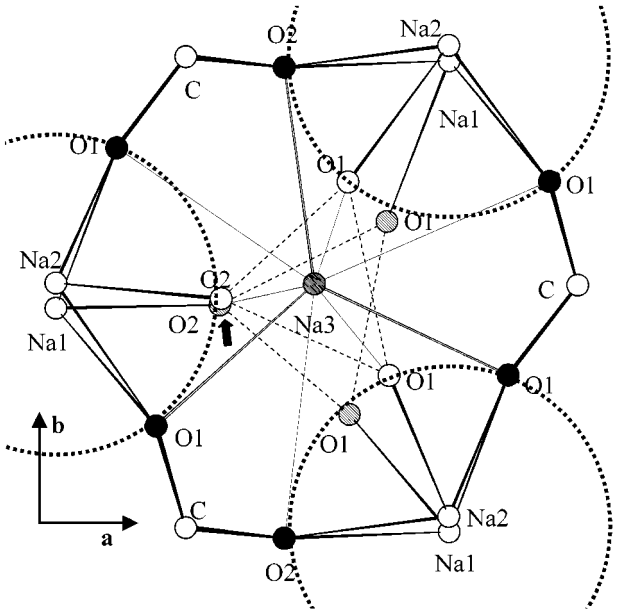

(*a*)

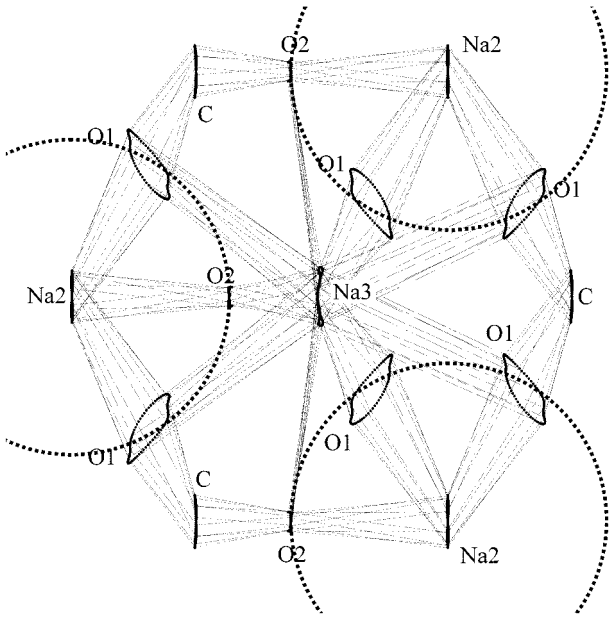

(*b*)

Figure 11
(*a*) Neighbourhood of ion $Na3^+$ in phase γ. The bonds to $Na3^+$ are plotted up to 3 Å; the double lines indicate bonds shorter than 2.5 Å. The middle CO_3^{2-} ions are indicated by dashed lines; the central C atoms are omitted. The O atoms of the lower CO_3^{2-} ion are hatched. The large dashed circles are cross sections of the NaO_6 columns. The black rings denote atoms that come in close contact (< 2.5 Å) with $Na3^+$ depending on the configuration of the modulated structure. They are however never simultaneously within this contact. The arrow shows the only O2 atom that permanently keeps a short contact with $Na3^+$. (*b*) The modulations of $Na3^+$ and its neighbourhood in phase γ. The bonds and positions are plotted with internal coordinate steps of 0.1 and 0.01, respectively. For clarity, $Na1^+$ ions are omitted. If two identical atoms, for instance O1,O1, differ by integer translation along **c**, their trajectories overlap.

Table 8
Comparison of refinements for the three structure models of δ-Na_2CO_3 derived from the superspace symmetry $C2/m(\alpha 0\gamma)0s$.

NW_{max} and NW_{used}: maximum and final number of waves for position and displacement modulation, respectively; *NP*: number of parameters; R_1, R_2 and S_1, S_2: *R* values and goodness-of-fit, respectively, for the superspace (subscript 1) and supercell (subscript 2) refinement; *NR*: number of reflections; *NA*: number of independent atoms in the sixfold supercell; 'fixed' lists the parameters that were fixed in addition to those fixed by symmetry. The cos terms of the *i*th modulation wave are denoted c,*i*.

t_0	Group	NW_{used}	NW_{max}	*NP*	R_1	S_1	*NR*	*NA*	R_2	S_2	Fixed
1/8	$P2_1/n$	6	6	326	0.0432	1.64	5695	36	0.0432	1.64	c,6 for all atoms
0	$P2/n$	6	6	330	0.0656	2.97	5695	38	0.0656	2.97	c,6 or s,6†
1/5	Pn	6	12	326	0.0435	1.65	5695	72	–	–	–
		11‡	12	619	0.0415	1.51	5695	72	0.0413§	1.48	–
		12	12	648	0.0483	1.75	9054	72	0.0483	1.75	c,12 for all atoms

† 12 waves could not be used due to computational problems. ‡ For refinement in the supercell a full set of 648 parameters was used. § s,6 for Na1 and Na2 because of their special symmetry positions.

In NaO_6 octahedra, the variation in Na—O distances is ∼0.05 Å, despite the fact that all participating atoms except O2 are strongly modulated (Fig. 9). On the other hand, the angles are subject to larger variations. A significant modulation occurs especially for Na—O1—O2 angles with minimal and maximal values varying from 12° for Na1 to 21° for Na2. The larger deformation of $Na2O_6$ octahedra is due to their locations, where the column of NaO_6 octahedra is strained. This is clearly visible in Fig. 8 by observing the lines connecting the O1 atoms.

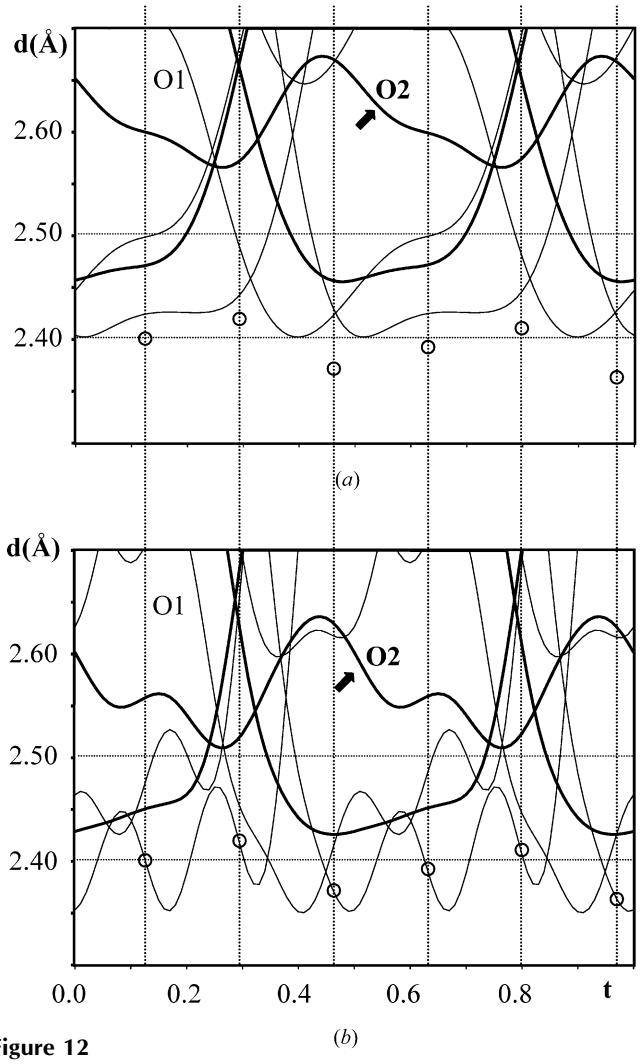

Figure 12
The Na3—O distances plotted as a function of the internal coordinate *t* for (*a*) γ- and (*a*) δ-sodium carbonate. Bold lines indicate Na3—O2 distances; other lines correspond to Na3—O1 distances. The distance indicated by the arrow is the only permanent contact. The vertical dotted lines indicate the values of *t* where the modulation functions of phase δ are defined. The open circles show the shortest distances found in phase δ.

5.4. The role of $Na3^+$ in phase transitions of sodium carbonate

In the main building units of sodium carbonate (CO_3 groups and NaO_6 octahedra) the influence of phase transitions on bond lengths is very low. The bending of columns and the corresponding change of angles in the octahedra can be understood in terms of the response to some external changes rather than the driving force of the phase transitions.

A different situation occurs with $Na3^+$ ions. This atom is located between CO_3^{2-} ions (Fig. 8) and is not part of the NaO_6 octahedra. In phase α the large Na3—O distances Na3—O (Table 15) cause the corresponding bond-valence sum to be much lower than 1 (Table 14). On the other hand, its bonding potential should be the same as for other Na atoms, although they are already bonded to all the O atoms available. In phase α the position of $Na3^+$ in the centre of a large hole is stabilized by thermal energy. In phase β the coordination of Na3 is more compact as a result of the shear-strain transition, but there is still no Na3—O bond as short as those occurring in NaO_6 octahedra.

The detail of the Na3 coordination in phase γ is shown in Fig. 11(*a*) for $t = 0$ and in Fig. 11(*b*) for the whole interval of internal coordinate *t* sampled in steps of 0.01. The bond-valence sums indicate that the average coordination is slightly closer than in phase β, but that the average Na3—O distances are indeed not too dissimilar. However, in some modulated configurations, $Na3^+$ exhibits close contacts with the neighbouring O atoms with bond lengths as short as in the NaO_6 octahedra. Fig. 12(*a*) shows the Na3—O distances in the γ phase plotted as a function of the internal coordinate *t*. The Na3—O contacts with bond lengths below 2.5 Å exist simultaneously for at most three atoms and are established sequentially with most of the coordinated O atoms. This behaviour is only possible because of the strongly modulated

Table 9
Final coordinates, equivalent isotropic displacement parameters and Fourier amplitudes of the displacive modulation functions of δ-Na_2CO_3.

The waves are sorted by the terms (s for sinus, c for cosinus) and n.

	Wave	x	y	z	U_{eq} (Å^2)
Na1		0	0	0	0.00886 (10)
	s,1	0	0.05944 (9)	0	
	c,1	0	0	0	
	s,2	0.00197 (6)	0	0.00150 (8)	
	c,2	0	0	0	
	s,3	0	−0.00826 (8)	0	
	c,3	0	0	0	
	s,4	−0.00264 (6)	0	−0.00214 (10)	
	c,4	0	0	0	
	s,5	0	0.00199 (8)	0	
	c,5	0	0	0	
	s,6	0.00189 (5)	0	0.00205 (8)	
	c,6	0	0	0	
Na2		0	0	0.5	0.00855 (10)
	s,1	0	0.06728 (9)	0	
	c,1	0	0	0	
	s,2	0.00096 (6)	0	−0.00230 (8)	
	c,2	0	0	0	
	s,3	0	0.00738 (8)	0	
	c,3	0	0	0	
	s,4	0.00104 (6)	0	−0.00030 (10)	
	c,4	0	0	0	
	s,5	0	0.00065 (8)	0	
	c,5	0	0	0	
	s,6	0.00121 (5)	0	0.00037 (8)	
	c,6	0	0	0	
Na3		0.17125 (4)	0.5	0.74784 (6)	0.01267 (8)
	s,1	0	0.07192 (7)	0	
	c,1	0	−0.00599 (7)	0	
	s,2	−0.00134 (4)	0	−0.00089 (6)	
	c,2	0.00141 (4)	0	0.00475 (6)	
	s,3	0	0.00253 (6)	0	
	c,3	0	−0.00640 (6)	0	
	s,4	0.00346 (5)	0	0.00228 (7)	
	c,4	0.00257 (5)	0	−0.00013 (8)	
	s,5	0	0.00174 (7)	0	
	c,5	0	−0.00219 (7)	0	
	s,6	0.00680 (7)	0	0.00216 (11)	
	c,6	0	0	0	
C		0.16454 (7)	0.5	0.24887 (10)	0.00695 (12)
	s,1	0	0.06120 (12)	0	
	c,1	0	−0.00040 (12)	0	
	s,2	0.00081 (9)	0	−0.00222 (13)	
	c,2	0.00111 (9)	0	−0.00141 (13)	
	s,3	0	0.00144 (12)	0	
	c,3	0	0.00855 (12)	0	
	s,4	−0.00055 (10)	0	−0.00001 (16)	
	c,4	0.00032 (10)	0	−0.00031 (16)	
	s,5	0	−0.00186 (15)	0	
	c,5	0	0.00072 (13)	0	
O1		0.10175 (5)	0.29345 (6)	0.28667 (7)	0.01312 (9)
	s,1	−0.02952 (6)	0.08019 (8)	−0.02347 (9)	
	c,1	−0.01883 (6)	0.00383 (8)	−0.03778 (8)	
	s,2	0.00108 (5)	0.00215 (7)	−0.00175 (8)	
	c,2	0.00052 (5)	−0.00005 (7)	−0.00252 (8)	
	s,3	0.00200 (6)	0.00106 (7)	0.00322 (8)	
	c,3	−0.00859 (5)	0.01515 (7)	−0.00367 (8)	
	s,4	0.00015 (6)	0.00112 (7)	0.00074 (9)	
	c,4	0.00072 (6)	0.00087 (7)	−0.00010 (9)	
	s,5	0.00335 (6)	−0.00466 (8)	0.00098 (10)	
	c,5	0.00068 (6)	0.00048 (7)	0.00081 (10)	
	s,6	−0.00139 (10)	−0.00226 (12)	−0.00282 (15)	
	c,6	0	0	0	
O2		0.28941 (6)	0.5	0.17472 (9)	0.01135 (11)
	s,1	0	0.02245 (12)	0	
	c,1	0	−0.00970 (12)	0	
	s,2	0.00083 (7)	0	−0.00297 (10)	
	c,2	0.00252 (7)	0	−0.00019 (10)	
	s,3	0	0.00345 (10)	0	
	c,3	0	−0.00461 (10)	0	
	s,4	−0.00152 (8)	0	−0.00069 (12)	
	c,4	−0.00020 (8)	0	−0.00183 (13)	
	s,5	0	0.00263 (11)	0	
	c,5	0	0.00241 (12)	0	
	s,6	0.00223 (9)	0	0.00320 (15)	
	c,6	0	0	0	

Na3 position and movement of NaO_6 octahedra, the latter being understood as a response to the tendency of $Na3^+$ to saturate its free bonding capacity. Despite the fact that the nearest O atoms alternate, the average bond-valence sum calculated for Na3—O distances up to 3.5 Å exhibits only small variation, ±0.05 (Fig. 13).

A closer look at Fig. 12(*a*) shows that only one of the Na3—O2 bonds remains present for all values of t, while other short contacts appear and disappear in various configurations of the modulations. The permanent bond is indicated by an arrow on Fig. 11(*a*). Its length reaches two minima at points $t \simeq 0.29$ and $t \simeq 0.79$, where only two short contacts under 2.5 Å appear, contrary to most other configurations where three such contacts exist. One short missing bond is compensated for not only by the minimum value of the above-mentioned Na3—O2 bond, but also by the presence of two other Na3—O2 bonds which are only 0.1 Å longer. Therefore, in this configuration Na3 is almost the same distance to O2 atoms as to all three neighbouring NaO_6 octahedra. An analysis of the shape of the column represented in Fig. 8 revealed that this occurs only when $Na3^+$ is located in the straight part of the column. Two additional points at $t \sim 0.25$ and 0.75 are characteristic (Fig. 12*a*). Here only one short Na—O bond exists, completed with four longer ones having almost the same length of 2.57 Å.

At the $\gamma \Rightarrow \delta$ transition, only the six most stable Na3O coordinations are selected. Considering that the points 0.29 and 0.79 are close to 1/8 + 1/6 and 1/8 + 4/6, the configuration with three nearly equal Na3—O2 bonds is also realised in the superstructure. On the other hand, the configurations with $t \simeq 0.25$ and 0.75 found in phase γ are absent in phase δ. All the remaining points (1/8, 1/8 + 2/6, 1/8 + 3/6 and 1/8 + 5/6) correspond to configurations where three Na3—O bonds shorter than 2.5 Å exist simultaneously. This is an indication that the phase transition $\gamma \Rightarrow \delta$ is also driven by the unsaturated $Na3^+$ ion. In Fig. 12(*b*) the Na3—O bonds of phase δ are plotted as a function of t and compared with phase γ. Here one should only focus on the definition points of the modulation functions. Outside, they acquire unreasonable values owing to the high number of harmonic waves used in the refinement. Comparison with the corresponding curves in phase γ shows that both structures are very close except for the overall decrease of the bond lengths.

The last feature to discuss is the influence of the $Na3^+$ ion on the size and shape of the NaO_6 octahedra. The permanent Na3—O2 bond mentioned above is the reason that all CO_3 groups are tilted in order to let O2 be nearer to $Na3^+$. This tilt

Table 10
Final displacement parameters and displacement modulation functions of δ-Na_2CO_3.

The waves are sorted by the terms (s for sinus, c for cosinus) and n.

	Wave	U^{11}	U^{22}	U^{33}	U^{12}	U^{13}	U^{23}
Na1		0.00927 (18)	0.00910 (12)	0.00885 (17)	0	0.00338 (15)	0
Na2		0.01018 (18)	0.00779 (11)	0.00831 (17)	0	0.00332 (15)	0
Na3		0.01204 (15)	0.01238 (10)	0.01448 (16)	0	0.00482 (13)	0
	s,1	0	0	0	−0.00003 (12)	0	−0.00085 (12)
	c,1	0	0	0	0.00195 (12)	0	0.00091 (13)
	s,2	0.00027 (19)	0.00072 (13)	−0.00036 (18)	0	−0.00029 (16)	0
	c,2	0.00016 (18)	0.00218 (13)	0.00043 (18)	0	0.00031 (15)	0
C		0.0071 (2)	0.00690 (14)	0.0072 (2)	0	0.00232 (19)	0
O1		0.01620 (17)	0.00969 (10)	0.01463 (16)	−0.00452 (10)	0.00584 (14)	0.00021 (10)
	s,1	−0.0015 (2)	0.00132 (13)	0.0009 (2)	−0.00144 (13)	−0.00038 (20)	−0.00036 (13)
	c,1	−0.0033 (2)	0.00100 (14)	0.0009 (2)	−0.00030 (14)	−0.0003 (2)	−0.00076 (14)
	s,2	−0.0018 (2)	−0.00139 (13)	−0.0019 (2)	0.00157 (14)	−0.00138 (19)	0.00115 (14)
	c,2	0.0012 (2)	0.00138 (13)	−0.0008 (2)	−0.00127 (14)	0.00005 (19)	−0.00082 (14)
	s,3	0.0010 (2)	−0.00033 (13)	0.0000 (2)	0.00002 (14)	0.0000 (2)	0.00045 (14)
	c,3	−0.0007 (2)	0.00094 (13)	0.0003 (2)	−0.00055 (14)	0.0000 (2)	−0.00027 (14)
	s,4	0.0000 (3)	−0.00117 (13)	0.0005 (3)	0.00119 (15)	0.0002 (2)	0.00040 (15)
	c,4	0.0000 (3)	0.00109 (14)	−0.0008 (3)	−0.00024 (15)	−0.0007 (2)	0.00039(15)
O2		0.00874 (19)	0.01506 (15)	0.0115 (2)	0	0.00509 (17)	0
	s,1	0	0	0	0.00253 (18)	0	0.00145 (19)
	c,1	0	0	0	−0.00059 (18)	0	0.00005 (19)
	s,2	−0.0003 (3)	−0.0014 (2)	−0.0007 (3)	0	0.0001 (2)	0
	c,2	−0.0008 (3)	0.0006 (2)	−0.0006 (3)	0	−0.0005 (2)	0

Table 11
The fit between observed and calculated data of δ-Na_2CO_3 for 5695 reflections exceeding the $3\sigma(I)$ limit using different sets of displacement modulation parameters in the refinement.

Models 1 and 2 use the full and reduced sets of parameters, while in model 3 the displacement modulation is not refined. R_1, R_2 and R_3: the R factors for first-, second- and third-order satellites, respectively; *NP*: number of parameters.

Model	S	R_{all}	R_{main}	R_1	R_2	R_3	*NP*
1	1.64	0.0428	0.0368	0.0383	0.0515	0.0624	326
2	1.71	0.0451	0.0384	0.0398	0.0549	0.0674	206
3	2.08	0.0586	0.0487	0.0556	0.0693	0.0817	134

is clearly visible in Fig. 8. As a side effect, the average Na1—O2 bond (see Table 13) is 0.1 Å shorter than Na2—O2 in phase γ and 0.05 Å in phase δ. The graphs illustrated in Fig. 13 seem to be in contradiction with this phenomenon as they show a smaller bond-valence sum for $Na1^+$ than for $Na2^+$. This difference appears for all configurations of phases γ and δ and indicates a slightly tighter coordination of $Na2^+$ compared with $Na1^+$. The tilt of the CO_3 groups brings not only O2 nearer to $Na1^+$, but also to $Na3^+$, as illustrated in Fig. 14. This is the reason why the Na1—O1 bonds are on average 0.05 Å longer that the corresponding Na2—O1 bonds. As the octahedra consist of four O1 and only two O2 atoms, the shorter Na1—O2 bonds are compensated with longer Na1—O1 bonds. The further increase of the bond-valence sum of $Na2^+$ is caused by the upper limit of 3.5 Å, within which another O atom appears for $Na2^+$, but not for $Na1^+$.

5.5. Modulation of displacement parameters

A closer look at the displacement parameters (see Table 5, Table 10 and Fig. 10) yields a very consistent model. In phase δ both the basic displacement parameters and their modulations are lower than in phase γ as a consequence of the lower temperature. The relative ADP modulation is the same in both phases, *i.e.* no modulation of C, little modulation of Na1 and Na2, and large modulation of O1, O2 and Na3. The large ADP modulation of Na3 is caused by its highly variable neighbourhood, while Na1 and Na2 with stable octahedral coordination exhibit virtually no ADP modulation. The same explanation is valid for atoms O1 and O2, because O2 with a weaker ADP modulation is permanently in contact with Na3, whereas O1 with a strong positional modulation is not (Fig. 12). The lower displacement parameters of O2 confirm our

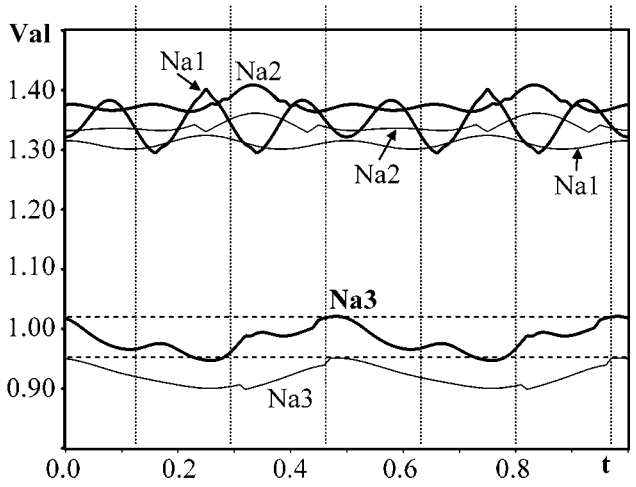

Figure 13
Bond-valence sums of sodium as a function of the internal coordinate t. Bold lines correspond to phase δ; the other lines are calculated for phase γ. The vertical dotted lines indicate values of t where the modulation functions of phase δ are defined.

Table 12
Final coordinates and equivalent isotropic displacement parameters of δ-Na_2CO_3 after transformation to the sixfold superstructure and refinement.

	x	*y*	*z*	U_{eq}
Na1*a*	0.00003 (4)	0.03491 (10)	−0.00021 (4)	0.0092 (3)
Na1*b*	0.49742 (4)	0.06370 (10)	0.16425 (5)	0.0093 (2)
Na1*c*	0.99974 (4)	0.01155 (10)	0.33290 (5)	0.0084 (2)
Na2*a*	−0.00038 (4)	0.05997 (10)	0.16675 (5)	0.0081 (2)
Na2*b*	0.49873 (4)	0.02327 (10)	0.33324 (5)	0.0090 (2)
Na2*c*	0.99989 (4)	−0.05239 (10)	0.49910 (4)	0.0088 (3)
Na3*a*	0.08609 (4)	0.54498 (11)	0.27874 (5)	0.0125 (3)
Na3*b*	0.58872 (4)	0.47163 (12)	0.44740 (5)	0.0134 (3)
Na3*c*	1.08713 (4)	0.42904 (11)	0.61010 (5)	0.0121 (3)
Na3*d*	−0.08099 (8)	0.4396 (2)	−0.27468 (10)	0.0125 (5)
Na3*e*	0.41465 (8)	0.5218 (2)	−0.11197 (10)	0.0139 (5)
Na3*f*	0.91453 (8)	0.5616 (2)	0.05597 (10)	0.0118 (5)
C*a*	0.08211 (7)	0.55578 (18)	0.11039 (8)	0.0064 (5)
C*b*	0.58224 (7)	0.53964 (18)	0.27756 (9)	0.0075 (5)
C*c*	1.08277 (7)	0.47325 (16)	0.44293 (8)	0.0071 (5)
C*d*	−0.08294 (7)	0.49655 (17)	−0.11028 (8)	0.0076 (5)
C*e*	0.41884 (7)	0.56417 (18)	0.05564 (9)	0.0066 (5)
C*f*	0.91759 (7)	0.54406 (17)	0.22324 (8)	0.0069 (5)
O1*a*	0.03693 (6)	0.36473 (18)	0.09896 (8)	0.0123 (4)
O1*b*	0.54969 (7)	0.33586 (20)	0.28544 (8)	0.0154 (5)
O1*c*	1.06487 (6)	0.25633 (18)	0.46323 (8)	0.0120 (4)
O1*d*	1.56444 (4)	0.22169 (11)	0.62640 (5)	0.0122 (3)
O1*e*	2.04989 (4)	0.24243 (12)	0.77149 (5)	0.0138 (3)
O1*f*	2.53734 (4)	0.33359 (11)	0.92626 (5)	0.0115 (3)
O1*g*	−0.06464 (9)	0.2804 (2)	−0.12994 (11)	0.0146 (5)
O1*h*	0.46436 (8)	0.3814 (2)	0.06108 (10)	0.0147 (5)
O1*i*	0.96338 (8)	0.3536 (2)	0.23796 (10)	0.0118 (5)
O1*j*	1.46126 (7)	0.30882 (18)	0.40518 (8)	0.0144 (5)
O1*k*	1.93445 (7)	0.20608 (18)	0.54412 (8)	0.0135 (5)
O1*l*	2.43402 (7)	0.23668 (18)	0.70332 (8)	0.0120 (5)
O2*a*	0.14454 (7)	0.52303 (19)	0.10646 (9)	0.0111 (5)
O2*b*	0.64588 (7)	0.52523 (17)	0.27575 (8)	0.0125 (5)
O2*c*	1.14580 (7)	0.49702 (17)	0.43988 (8)	0.0109 (5)
O2*d*	−0.14541 (6)	0.51710 (19)	−0.10580 (8)	0.0109 (4)
O2*e*	0.35792 (7)	0.51566 (19)	0.06112 (8)	0.0124 (5)
O2*f*	0.85551 (6)	0.51497 (18)	0.22787 (8)	0.0109 (4)

structure models with very low position modulation. Otherwise, it would try to deviate from the stable position by means of large displacement parameters.

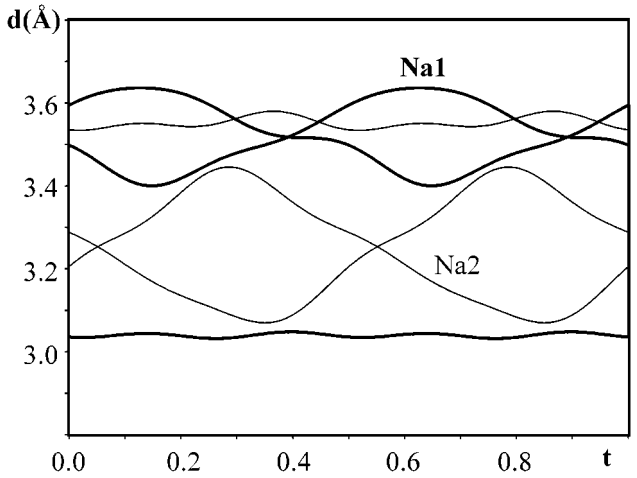

Figure 14
The distances Na3—Na1 (bold lines) and Na3—Na2 (thin lines) plotted as a function of the internal coordinate *t*.

Table 13
Selected bond distances (Å) and angles (°).

γ_h denotes phase γ refined in the harmonic approximation. The data for phases α and β are taken from Swainson *et al.* (1995).

		Min.	Max.	Average
C—O1	α	–	–	1.187 (3)
	β	–	1.225 (5)	
	γ	1.274 (3)	1.286 (3)	1.281 (3)
	γ_h	1.249 (2)	1.308 (2)	1.282 (2)
	δ	1.287 (3)	1.292 (3)	1.290 (3)
C—O2	α	–	–	1.187 (3)
	β	–	–	1.293 (8)
	γ	1.278 (2)	1.288 (2)	1.283 (2)
	γ_h	1.278 (2)	1.291 (2)	1.285 (2)
	δ	1.288 (3)	1.293 (3)	1.291 (3)
O1—C–O1	γ	118.9 (2)	120.1 (2)	119.6 (2)
	γ_h	119.1 (1)	120.9 (1)	120.0 (1)
	δ	119.2 (2)	119.9 (2)	119.6 (2)
O1—C—O2	γ	119.9 (2)	120.6 (2)	120.2 (2)
	γ_h	119.1 (1)	120.6 (2)	120.0 (2)
	δ	119.9 (2)	120.6 (2)	120.2 (2)
Na1—O1	α	–	–	2.441 (3)
	β	–	–	2.420 (4)
	γ	2.334 (2)	2.434 (2)	2.377 (2)
	γ_h	2.342 (1)	2.448 (1)	2.379 (1)
	δ	2.330 (2)	2.424 (2)	2.367 (3)
Na1—O2	β	–	–	2.333 (5)
	γ	2.319 (2)	2.362 (2)	2.340 (2)
	γ_h	2.337 (1)	2.343 (1)	2.340 (1)
	δ	2.308 (2)	2.365 (2)	2.367 (3)
Na2—O1	β	–	–	2.350 (4)
	γ	2.295 (3)	2.351 (3)	2.326 (3)
	γ_h	2.309 (2)	2.360 (2)	2.328 (2)
	δ	2.297 (3)	2.349 (3)	2.318 (3)
Na2–O2	β	–	–	2.484 (4)
	γ	2.416 (2)	2.447 (2)	2.435 (2)
	γ_h	2.425 (1)	2.445 (1)	2.435 (1)
	δ	2.395 (2)	2.428 (2)	2.415 (2)

Table 14
Bond-valence sums according to Brown & Altermatt (1985), in sodium carbonate calculated up to 35 Å for phases α, β, γ and δ.

In phase α the atoms Na1, Na2 and O1, O2 are symmetrically equivalent. In phases γ and δ, the average values are given.

	α	β	γ	δ
Na1	1.06	1.26	1.34	1.38
Na2	–	1.25	1.36	1.40
Na3	0.71	0.80	0.94	1.00
C	5.20	4.43	4.04	3.95
O1	2.15	2.03	1.89	1.88
O2	–	1.79	1.88	1.89

5.6. The harmonic and anharmonic descriptions of phase γ

In our refinement of phase γ, satellites and modulation waves of up to fourth order have been used. A comparison with the results of the harmonic refinement using only first-order satellites and one harmonic modulation wave reveals that the overall features of the structure are not changed. However, both models differ in details. The CO_3 group is less rigid in the harmonic approximation: the fluctuations are 0.06 Å for bond lengths and 2° for angles, which is in agreement with the values given by de Wolff & Tuinstra (1986).

Table 15
Na3—O distances calculated up to 35 Å for various phases of sodium carbonate.

In phase α atoms O1 and O2 are equivalent. In the average phase γ, the minimum and maximum distances are listed. In the δ phase atoms Na3, O1 and O2 split to many symmetry-independent positions; all possible distances in the commensurate model can be described using two positions of Na3.

	α	β	γ	δ	
O1	2.624	2.575	2.597 (2.402 2.835)	2.567 (2.406 2.721)	2.606 (2.403 2.865)
O1	2.624	2.575	2.600 (2.402 2.835)	2.567 (2.406 2.721)	2.606 (2.403 2.865)
O1	2.624	2.680	2.632 (2.402 2.906)	2.663 (2.377 2.972)	2.614 (2.370 2.937)
O1	2.624	2.680	2.636 (2.402 2.906)	2.663 (2.377 2.972)	2.614 (2.370 2.937)
O1	2.624	3.064	2.959 (2.646 3.244)	2.943 (2.619 3.238)	2.916 (2.599 3.205)
O1	2.624	3.064	2.964 (2.646 3.244)	2.943 (2.619 3.238)	2.916 (2.599 3.205)
O2	3.461	2.719	2.615 (2.566 2.673)	2.569 (2.518 2.632)	2.567 (2.535 2.603)
O2	3.461	2.668	2.671 (2.456 2.907)	2.664 (2.426 2.918)	2.678 (2.453 2.919)
O2	3.461	2.668	2.675 (2.456 2.907)	2.664 (2.426 2.918)	2.678 (2.453 2.919)
O2	3.461	–	–	–	–
O2	3.461	–	–	–	–
O2	3.461	–	–	–	–

Obviously the harmonic refinement tends to compensate the electron density maxima of the anharmonic movement of the group with the help of oxygen positions. On the other hand, there is no difference between the rigidity of the distances in NaO_6 octahedra. In both cases, the fluctuation of the Na—O bonds is ~ 0.05 Å. If we follow the shape of the NaO_6 columns (Fig. 8) as a line connecting atoms Na1 and Na2, there is no visible difference between both descriptions. The rather sharp turns of the line are achieved by combining two harmonic functions for Na1 and Na2.

The coordination distances of $Na3^+$ based on the harmonic refinement are plotted in Fig. 15. A comparison with Fig. 12(*a*) shows important contrasts. First, the permanent Na3—O2 bond exhibits virtually no modulation in the harmonic model, while in the anharmonic model it shows strong minima and maxima corresponding to the definition points of phase δ. On the other hand, the values of t for which $Na3^+$ shares approximately three equal bonds to the neighbouring O2 atoms are the same in both phases. Another difference can be observed in the intervals of t where $Na3^+$ creates three short bonds below 2.5 Å. The intervals still contain the definition points of phase δ, but they are shorter than in the anharmonic description. Moreover, the Na3—O1 distance is sometimes smaller than the 2.40 Å limit that is strictly kept for the $Na3^+$ ion in both phases δ and (anharmonically described) γ. It appears that the anharmonic description is fundamental to the understanding of the behaviour of $Na3^+$.

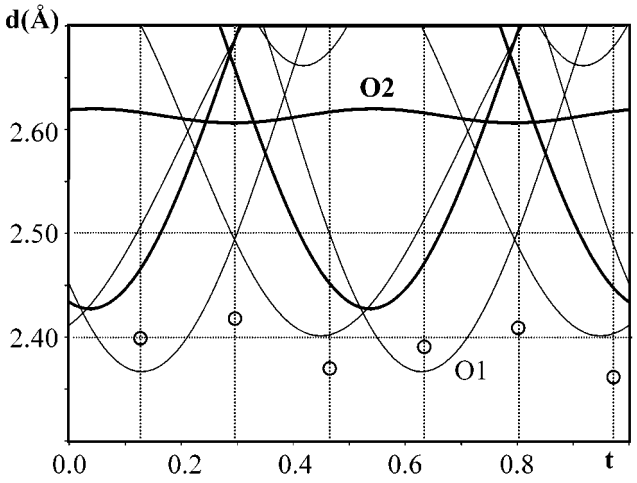

Figure 15
The distances Na3—O plotted as a function of the internal coordinate t for phase γ refined in the harmonic approximation. The bold lines are Na3—O2 distances; the other lines correspond to Na3—O1 distances. The vertical dotted lines indicate values of t where the modulation functions of phase δ are defined. The open circles show the shortest distances found in phase δ.

6. Conclusions

In the present work we have completed the structure analysis of γ-sodium carbonate which was started almost 30 years ago during the opening of a new exciting field of aperiodic crystallography. Based on the progress in experimental and computing techniques, we could use higher-order satellites and additional harmonic modulation waves to model the anharmonic features of the structure. Our new model agrees with the main features of the harmonic description. However, it reveals a more detailed view necessary to the understanding of the factors leading finally to the commensurate low-temperature phase δ.

For the first time we present the structure analysis of phase δ. The unified superspace description contributed greatly to the comparison of both phases with very similar structure. The most significant differences were detected in the coordination of the $Na3^+$ ion. We found strong arguments for the hypothesis that this atom is aiming at the saturation of its free bonding capacity, which may be the driving force for phase transitions in sodium carbonate.

In the first place we gratefully mention Erwin Lam, Kurt Schenk, Naomi Furrer and Euro Solari. Without their experience the difficult task of single-crystal preparation could not have been realised. We thank Vaclav Petricek and Henrik Birkendal for valuable discussions and Andreas Schönleber for helping with the measurements. We gratefully acknowledge the support of the Swiss National Science Foundation (grants 20-56870.99) and the Grant Agency of the Czech Republic (grant 202/03/0430).

References

Aalst, W. van, den Hollander, J., Peterse, W. J. A. M. & de Wolff, P. M. (1976). *Acta Cryst.* B**32**, 47–58.

Bagautdinov, B., Pilz, K., Ludecke, J. & van Smaalen, S. (1999). *Acta Cryst.* B**55**, 886–895.
Brouns, E., Visser, J. W. & de Wolff, P. M. (1964). *Acta Cryst.* **17**, 614.
Brown, I. D & Altermatt, D. (1985). *Acta Cryst.* B**41**, 244–247.
Dam, B. & Janner, A. (1986). *Acta Cryst.* B**42**, 69–77.
Evain, M., Boucher, F., Gourdon, O., Petricek, V., Dusek, M. & Bezdicka, P. (1998). *Chem. Mater.* **10**, 3068–3076.
Harris, M. J. & Dove, M. T. (1995). *Mod. Phys. Lett. B*, **9**, 67–85.
Harris, M. J., Dove, M. T. & Godfrey, K. W. (1996). *J. Phys. Condens. Matter*, **8**, 7073–7084.
Harris, M. J. & Salje, E. K. H. (1992). *J. Phys. Condens. Matter*, **4**, 4399–4408.
Kuma Diffraction (2000). *RED* Version 1.168. Kuma Diffraction Instruments GmbH, Wroclaw, Poland.
Lam, E. J. W. (1998). Unpublished results.
Lambert, S., Leligny, H., Grebille, D., Pelloquin, D. & Raveau, B. (2002). *Chem. Mater.* **14**, 1818–1826.
Meyer, M., Paciorek, W., Schenk, K. & Chapuis, G. (1995). *Proceedings of the International Conference on Aperiodic Crystals (Aperiodic '94)*, Les Diablerets, Switzerland, pp. 483–487. Singapore: World Scientific.
Oxford Diffraction (2001). *RED*, Version 1.169.2. Oxford Diffraction, Oxford, UK.
Pater, C. J. de & Helmholdt, R. B. (1979). *Phys. Rev. B*, **19**, 5735–5745.
Petricek, V. & Dusek, M. (2000). *JANA*2000. Institute of Physics, Praha, Czech Republic.
Schönleber, A., Meyer, M. & Chapuis, G. (2001). *J. Appl. Cryst.* **34**, 777–779.
Swainson, I. P., Dove, M. T. & Harris, M. J. (1995). *J. Phys. Condens. Matter*, **7**, 4395–4417.
Wolff, P. M. de (1974). *Acta Cryst.* A**30**, 777–785.
Wolff, P. M. de & Tuinstra, F. (1986). *Incommensurate Phases in Dielectrics 2*, 253–281. Amsterdam: Elsevier Science Publishers BV.